PHYSICAL REVIEW E **92**, 020401(R) (2015)

Local load-sharing fiber bundle model in higher dimensions

Santanu Sinha,[1,2,*] Jonas T. Kjellstadli,[2,†] and Alex Hansen[2,‡]
[1]*Department of Physics, University of Oslo, P.O. Box 1048, Blindern, N-0316 Oslo, Norway*
[2]*Department of Physics, Norwegian University of Science and Technology, N-7491 Trondheim, Norway*
(Received 27 February 2015; published 5 August 2015)

We consider the local load-sharing fiber bundle model in one to five dimensions. Depending on the breaking threshold distribution of the fibers, there is a transition where the fracture process becomes localized. In the localized phase, the model behaves as the invasion percolation model. The difference between the local load-sharing fiber bundle model and the equal load-sharing fiber bundle model vanishes with increasing dimensionality with the characteristics of a power law.

DOI: 10.1103/PhysRevE.92.020401 PACS number(s): 46.50.+a, 62.20.M−, 81.40.Np

The fiber bundle model has come a long way since its introduction in 1926 by Peirce [1]. Initially introduced to model the strength of yarn, the model has slowly gained ground as a model for fracture in somewhat the same way that the Ising model has become a paradigm for magnetic systems. In 1945, Daniels' paper [2] on the fiber bundle model led to a continuous interest for the model in the mechanics community. The statistical physics community became aware of the model in the early 1990s in the aftermath of the surge of interest in fracture and in that community [3,4].

The Peirce fiber bundle model is today known as the equal load-sharing (ELS) fiber bundle model. In this model N Hookean springs—fibers—of length x_0 and spring constant κ are placed between two parallel infinitely stiff clamps. When the distance between the clamps is $x_0 + x$, each fiber carries a load $\sigma = \kappa x$. Each fiber i has a maximum elongation threshold x_i, drawn from a probability density $p(x_i)$, up to which it can be sustained before failing permanently. So the corresponding maximum load it can sustain is therefore $\sigma_i = \kappa x_i$. When a fiber fails, its load is shared equally among the surviving fibers since the clamps are infinitely stiff, hence equal load sharing.

The local load-sharing (LLS) fiber bundle model was introduced by Harlow and Phoenix [5,6] as a one-dimensional array of fibers, each having an independent breaking threshold drawn from some threshold distribution $p(x)$. They defined the force redistribution rule as follows: When a fiber fails, the load it carried is redistributed in equal portions onto its two nearest surviving neighbors. Hence, if a fiber i is adjacent to $n_{l,i}$ failed fibers to the left and $n_{r,i}$ failed fibers to the right, it will carry a load [7]

$$\sigma_i = \kappa \left[1 + \frac{n_{l,i} + n_{r,i}}{2} \right] x, \tag{1}$$

where x is the distance between the clamps if all fibers were intact [4].

Whereas the ELS fiber bundle model is extreme in the sense that it redistributes the force carried by the failed fibers equally among all surviving fibers wherever they are placed, the LLS fiber bundle model is extreme in the opposite sense: Only the nearest survivors pick up the force carried by the failed fiber. There are many models that are intermediate between the two extreme models. For example, the γ model of Hidalgo *et al.* [8] distributes the force carried by the failed fiber according to a power law in the distance from the failed fiber. The soft clamp model [9–12] replaces one of the infinitely stiff clamps in the ELS model by a clamp with finite elastic constant. Hence, the load redistribution is governed by the elastic response of the soft clamp.

We emphasize the following subtle point in the implementation of the LLS model [4]. If the redistribution of forces after the failure of a fiber proceeds by dividing the force it carried in two and adding each half to the two nearest surviving fibers to the left and right, i.e., according to the recipe of Harlow and Phoenix [5], the force distribution will not follow Eq. (1). Rather, it will become dependent on the order in which the fibers have failed. Hence, it will not be possible to determine the force distribution among the fibers only from the knowledge of the present failed fibers in the system. This history dependence in the force distribution is unphysical. As an example, if two adjacent fibers have failed and the two nearest surviving fibers each has one survivor, the procedure will produce the following load distribution: (7/4,0,0,9/4) or (9/4,0,0,7/4) depending on the order in which the two middle fibers failed. According to Eq. (1), the load distribution should be (2,0,0,2) independent of the order in which the fibers failed.

When implementing the LLS model in two or more dimensions, the force redistribution algorithm becomes even more crucial. We insist that the model should be physical where the force distribution among the surviving fibers can be determined by only knowing which fibers have already failed and it should not depend on the order in which they have failed. This leads to the concept of clusters of failed fibers, where the term cluster is used in the same sense as in the site percolation problem [13]: Failed fibers that are nearest neighbors to each other form a cluster. The total load carried by all the failed fibers in a given cluster will then be shared equally by the surviving fibers that form the perimeter to that cluster. If a surviving fiber is adjacent to two different clusters of failed fibers, the total load it carries is the sum of the loads contributed from both the clusters.

This generalization of the one-dimensional LLS model to higher dimensions is the simplest one that ensures history independence in the force distribution. A more elaborate generalization may be found in Ref. [14]. Here one of the

*santanu.sinha@ntnu.no
†jonastk@stud.ntnu.no
‡alex.hansen@ntnu.no

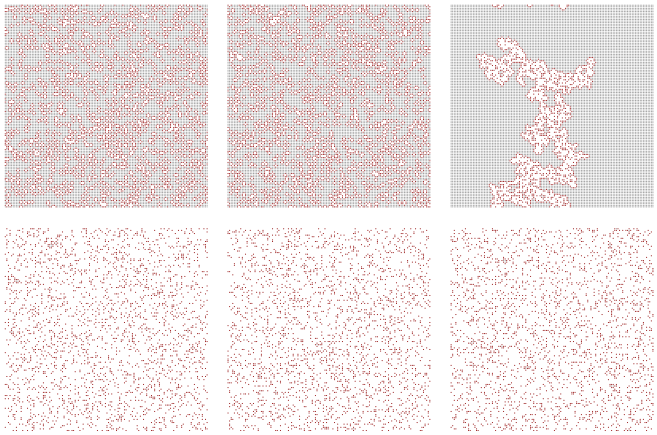

FIG. 1. (Color online) Snapshots of the two-dimensional LLS model after 1792 failed fibers (top row) and after 13 824 failed fibers (bottom row) with different threshold distributions for a 128×128 system. The red fibers are survivors adjacent to clusters of failed fibers, the gray fibers are survivors that are not adjacent to failed fibers, and white fibers have failed.

clamps is exchanged for a stretchable membrane that has no bending resistance. The elastic response of this model is equivalent to the LLS model in one dimension. However, it differs from the one we propose here in two dimensions.

We show in Fig. 1 the two stages of the two-dimensional LLS model: after 1792 (top row) and after 13 824 (bottom row) failed fibers. Here $N = 128^2$ fibers, placed at the sites of a square lattice with periodic boundary conditions in all directions, are seen from above. The failed fibers are shown as white, the intact fibers that belong to the external and internal perimeters of the clusters of failed fibers are shown as red, and other intact fibers are shown as gray. In the first column of the figure, the threshold distribution $p(x)$ was uniform on the unit interval. Hence, the cumulative probability was $P(x) = x$, where $x \in [0,1]$. In the next two columns, the cumulative threshold probability was $P(x) = 1 - \exp(x_< - x)$, where $x \in [x_<, \infty)$ with $x_< = 0$ and $x_< = 1$ respectively. In the top row it is hard to distinguish the difference between the first two panels of the figure. However, the third panel in the top row is very different. In this case, the breakdown process is *localized* from the very beginning. That is, a single cluster of failed fibers forms and keeps growing. On the other hand, the three panels in the bottom row are all very similar.

When the breakdown process is localized so that only one cluster of failed fibers forms, the model is equivalent to the invasion percolation model [15]. In the invasion percolation model, each site is given a random number. An initial site is invaded. The perimeter of this one-site cluster forms the growth sites and the growth site with the smallest random number associated with it is invaded. This is repeated, letting the perimeter of the cluster of invaded sites be the growth sites. In the LLS model, the perimeter of the single cluster of failed fibers will carry the extra force that makes these and only these fibers liable for failure when the threshold is narrow enough to imply localization. It will be the fiber in the perimeter that has the smallest failure threshold that will fail next. Hence, it behaves precisely as the invasion percolation model.

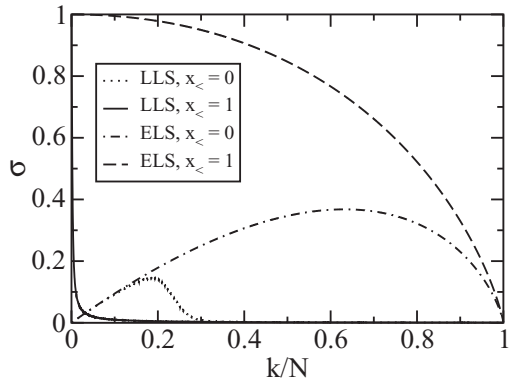

FIG. 2. Force per fiber σ as a function of the relative number of failed fibers k/N in the one-dimensional local load-sharing model together with the ELS model result (5). The thresholds were distributed according to $p(x) = \exp(-x + x_<)$, where $x \in [x_<, \infty)$ with $x_< = 0$ and 1, respectively. Here $N = 4000$. Each data series is based on 2000 samples.

We now consider the breaking characteristics of the LLS model in comparison to the ELS model. When k fibers have failed, the force F carried by the surviving fibers in the ELS model is

$$F = N\sigma = (N-k)\kappa x, \tag{2}$$

where we have defined the applied force per fiber $\sigma = F/N$. In the LLS model we have

$$F = N\sigma = N\kappa x, \tag{3}$$

since the surviving perimeter fibers precisely absorb the load carried by the failed fibers.

We order the failure thresholds of the N fibers in an ascending sequence $x_{(1)} < x_{(2)} < \cdots < x_{(k)} < \cdots < x_{(N)}$. According to order statistics [16], the average (over samples) of the kth member of this sequence is given by

$$P(\langle x_{(k)} \rangle) = \frac{k}{N} \tag{4}$$

for large N. We combine this equation with Eq. (2) for the ELS model assuming that $P(x) = 1 - \exp(-x + x_<)$ for $x \in [x_<, \infty)$ to find

$$\sigma = \kappa \left[1 - \frac{k}{N}\right]\left[x_< - \ln\left(1 - \frac{k}{N}\right)\right]. \tag{5}$$

For a uniform threshold distribution in $[x_<, 1]$, the cumulative probability is $P(x) = (x - x_<)/(1 - x_<)$ and we find

$$\sigma = \kappa \left[1 - \frac{k}{N}\right]\left[x_< + (1 - x_<)\frac{k}{N}\right]. \tag{6}$$

We show the ELS behavior for the exponential threshold distribution (5) in Fig. 2 together with the corresponding curves ($x_< = 0$ and $x_< = 1$) for the LLS model in one dimension. There is a large difference between the ELS and LLS models.

This picture changes in two dimensions. In Fig. 3 we show the results for the two-dimensional LLS model for exponential threshold distribution with cumulative threshold probabilities $P(x) = 1 - \exp(x_< - x)$, where $x \in [x_<, \infty)$ with $x_< = 0$ and 1. When comparing this figure to the corresponding one for

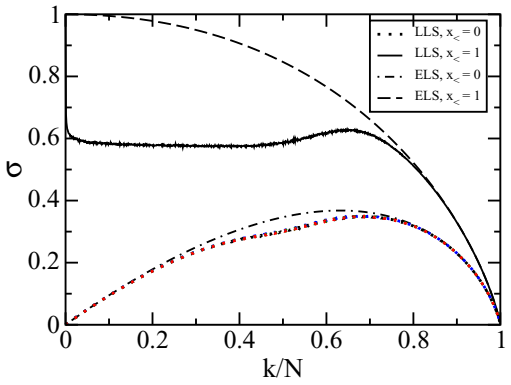

FIG. 3. (Color online) Force per fiber σ as a function of the relative number of failed fibers k/N in the two-dimensional LLS model compared with the ELS model result. The threshold distribution was $p(x) = \exp(x_< - x)$, where $x \in [x_<,\infty)$ with $x_< = 0$ and 1. The LLS results for $x_< = 0$ (the lowermost curve) are also compared for different system sizes $N = 32^2$ (blue), 64^2 (green), 128^2 (red), and 256^2 (black) and they fall exactly on each other, showing that the results are free from finite-size effects. For $x_< = 1$, $N = 256^2$. Each data series is based on 5000 samples.

one dimension (Fig. 2), we see that the LLS model now is much closer to the ELS model than in one dimension.

It should be pointed out that σ vs k/N for the exponential threshold distribution with $x_< = 1$ has a curious upward bend before its maximum value (see Fig. 3). We have also observed a small upward bend for the uniform threshold distribution with $x_< = 0.4$. This means that the model is stable in this region in the sense that if σ is used as the control parameter, fiber failures will only occur if σ is increased. This is not true in the ELS model. Hence, the LLS model is in fact *more stable* than the ELS model in this region.

The similarity between the ELS and LLS models is also evident in other quantities that characterize the two models. In Fig. 4 we show the burst distribution for the LLS model in two dimensions for the cumulative threshold probability $P(x) = 1 - \exp(x_< - x)$, where $x \in [x_<,\infty)$ with $x_< = 0$ and 1. The burst distribution is the histogram of the number of simultaneously failing fibers Δ when the force σ is the control parameter. Hemmer and Hansen showed in 1992 that the burst

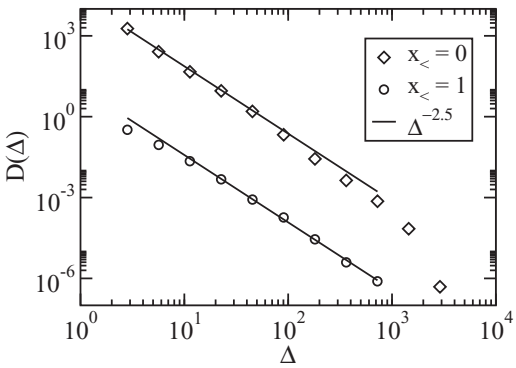

FIG. 4. Burst distribution in the two-dimensional LLS model. The threshold distribution was $p(x) = \exp(x_< - x)$, where $x \in [x_<,\infty)$. The data sets are based on 5000 samples of size $N = 256^2$.

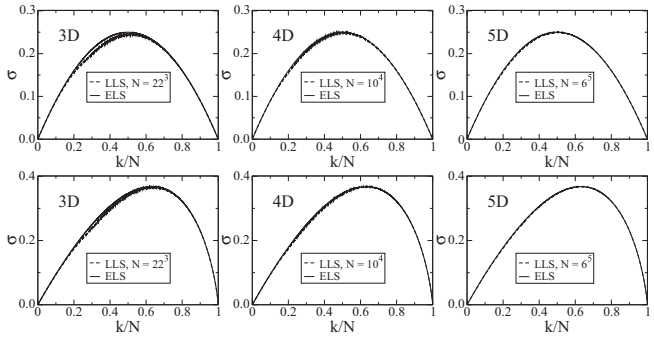

FIG. 5. Force per fiber σ as a function of the relative number of failed fibers k/N in the three-dimensional (3D), four-dimensional (4D), and five-dimensional (5D) LLS model. The top row corresponds to $P(x) = x$ with $x \in [0,1]$ and bottom row corresponds to $P(x) = 1 - \exp(x_< - x)$ with $x \in [x_<,\infty)$. Each data series is averaged over at least 40 000 samples.

distribution in the ELS model is given by

$$\omega(\Delta) \sim \Delta^{-5/2} \tag{7}$$

for a very wide class of threshold distributions to which $p(x) = \exp(x_< - x)$ belongs [17].

Later, Hansen and Hemmer investigated the burst distribution in the one-dimensional LLS model, finding a burst exponent ≈4.5 rather than 5/2 [18]. Kloster *et al.* [7] showed analytically that the burst distribution falls off faster than a power law in the LLS model when the threshold distribution is uniform on the unit interval. Figure 4 shows that the burst distribution in the two-dimensional LLS model is consistent with Eq. (7) for $p(x) = \exp(x_< - x)$, where $x_< = 0$ or $x_< = 1$.

In Fig. 5 we show the σ vs k/N curves for the three-dimensional, four-dimensional, and five-dimensional LLS fiber bundle models for the cumulative threshold probability $P(x) = x$ with $x \in [0,1]$ (top row) and $P(x) = 1 - \exp(x_< - x)$ with $x \in [x_<,\infty)$ (bottom row). We compare the curves with the ELS model results given in Eqs. (5) and (6). Interestingly, the curves for the LLS and the ELS models are approaching each other more and more as the dimensionality is increased. The difference in σ for the LLS and ELS models for different system dimensions is measured and plotted in Fig. 6 for the two threshold distributions.

It can be noticed that the maxima of the $\Delta\sigma$ curves shift towards smaller k/N with changing dimensionality. Therefore,

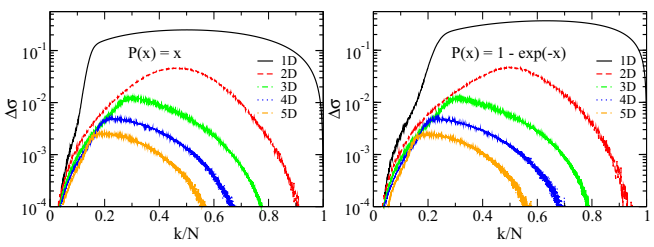

FIG. 6. (Color online) Difference between the force per fiber σ in the LLS and ELS models in one to five dimensions for the two threshold distributions. A rapid decrease in $\Delta\sigma$ can be observed with increasing dimensionality.

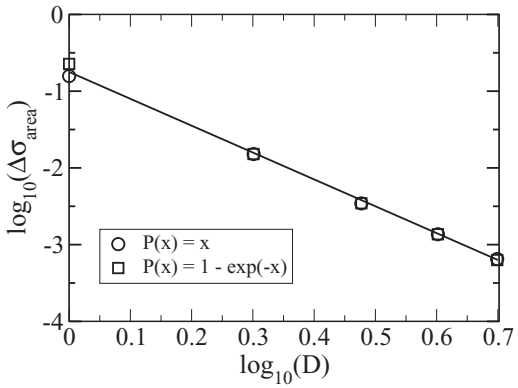

FIG. 7. Area under the $\Delta\sigma$ curves in Fig. 6 as a function of dimensionality D for the two different threshold distributions. The system sizes considered for one to five dimensions are 4000, 256^2, 22^3, 10^4, and 6^5 respectively.

in order to quantify the difference between the LLS and ELS models, we measure the total area $\Delta\sigma_{\text{area}}$ under the $\Delta\sigma$ curves. In Fig. 7 we plot $\Delta\sigma_{\text{area}}$ as a function of the dimensionality D of the system. Interestingly, a power-law dependence

$$\Delta\sigma_{\text{area}} \sim D^{-\mu}, \tag{8}$$

with $\mu = 3.5 \pm 0.1$, is observed. In the cases where the threshold cutoff is $x_< > 0$, there is a non-negligible N dependence in the σ vs k/N curves and the effective exponent μ needs further finite-size scaling analysis to be determined. From Eq. (8) we conclude that there is no finite upper critical dimension for which the LLS and ELS models become equal. However, the difference falls off rapidly with increasing D.

Why is there convergence between the LLS and ELS models with increasing dimensionality? Early in the breakdown process in the LLS model, fibers fail not due to being under stress because they are on the perimeter of clusters of already failed fibers, but because they have small thresholds. This is the same mechanism as in the ELS model. Hence, early on, the processes are similar, even in one dimension. As the breakdown process proceeds, the clusters of failed fibers merge and undergo a percolation transition. Essentially, all the remaining fibers become part of the perimeter of a single percolating cluster of failed fibers, which can be seen in the bottom row of Fig. 1. Hence, as all the remaining fibers are adjacent to the same cluster, they share the same force as in the ELS fiber bundle model and the breakdown process becomes similar again. The percolation transition occurs earlier in the breakdown process with increasing dimensionality as in standard percolation [13]. Therefore, as the dimensionality increases, the ELS and the LLS models must converge as the dimension is increased.

The LLS model is extreme in that it is the perimeter fibers that absorb the forces from the failed fibers. We have mentioned models that are in between the ELS and LLS models. When the LLS and ELS models are rapidly approaching each other with increasing D, so will the in between models; they will rapidly approach the ELS model with increasing D. This argument also applies to models that normally are not classified as fiber bundle models, such as the fuse model, for which Zapperi *et al.* [19] have reported a burst distribution exponent in three dimensions equal to 2.55, close to the ELS value 5/2. Hence, already in three dimensions, the ELS model is not far from the much more complex models of fracture.

We thank Per Christian Hemmer and Srutarshi Pradhan for numerous discussions about this subject. S.S. thanks the Research Council of Norway for support through Grant No. 216699.

[1] F. T. Peirce, J. Text. Ind. **17**, 355 (1926).
[2] H. E. Daniels, Proc. R. Soc. London Ser. A **183**, 405 (1945).
[3] S. Pradhan, A. Hansen, and B. K. Chakrabarti, Rev. Mod. Phys. **82**, 499 (2010).
[4] A. Hansen, P. C. Hemmer, and S. Pradhan, *The Fiber Bundle Model* (Wiley-VCH, Berlin, 2015).
[5] D. G. Harlow and S. L. Phoenix, J. Compos. Mater. **12**, 195 (1978).
[6] D. G. Harlow and S. L. Phoenix, J. Mech. Phys. Solids **39**, 173 (1991).
[7] M. Kloster, A. Hansen, and P. C. Hemmer, Phys. Rev. E **56**, 2615 (1997).
[8] R. C. Hidalgo, Y. Moreno, F. Kun, and H. J. Herrmann, Phys. Rev. E **65**, 046148 (2002).
[9] G. G. Batrouni, A. Hansen, and J. Schmittbuhl, Phys. Rev. E **65**, 036126 (2002).
[10] A. Stormo, K. S. Gjerden, and A. Hansen, Phys. Rev. E **86**, R025101 (2012).
[11] K. S. Gjerden, A. Stormo, and A. Hansen, Phys. Rev. Lett. **111**, 135502 (2013).
[12] K. S. Gjerden, A. Stormo, and A. Hansen, Front. Phys. **2**, 66 (2014).
[13] D. Stauffer and A. Aharony, *Introduction to Percolation Theory* (Taylor & Francis, London, 1994).
[14] S. Patinet, D. Vandembroucq, A. Hansen, and S. Roux, Europ. J. Phys. Spec. Top. **223**, 2339 (2014).
[15] D. Wilkinson and J. F. Willemsen, J. Phys. A **16**, 3365 (1983).
[16] E. J. Gumbel, *Statistics of Extremes* (Dover, Mineola, 2004).
[17] P. C. Hemmer and A. Hansen, ASME J. Appl. Mech. **59**, 909 (1992).
[18] A. Hansen and P. C. Hemmer, Phys. Lett. A **184**, 394 (1994).
[19] S. Zapperi, P. K. V. V. Nukala, and S. Šimunović, Physica A **357**, 129 (2005).